



Trend analysis of the airborne fraction and sink rate of anthropogenically released CO₂

Mikkel Bennedsen^{1,3}, Eric Hillebrand^{1,3}, and Siem Jan Koopman^{2,3}

¹Department of Economics and Business Economics, Aarhus University, Fuglesangs Allé, 4 8210 Aarhus V, Denmark

²Department of Econometrics, School of Business and Economics, Vrije Universiteit Amsterdam, De Boelelaan 1105, 1081 HV Amsterdam, The Netherlands.

³Center for Research in Econometric Analysis of Time Series (CREATES), Aarhus University, Fuglesangs Allé, 4 8210 Aarhus V, Denmark

Correspondence: Mikkel Bennedsen (mbennedsen@econ.au.dk)

Abstract. Is the fraction of anthropogenically released CO₂ that remains in the atmosphere increasing? Is the rate at which the ocean and land sinks take up CO₂ from the atmosphere decreasing? We analyze these questions by means of a statistical dynamic multivariate model from which we estimate the unobserved trend processes together with the parameters that govern them. By assuming a balanced global carbon budget, we obtain more than one data series to measure the same object (for example, the airborne fraction). Incorporating these additional data into the dynamic multivariate model in effect increases the number of available observations, thus improving the reliability of parameter estimates. We find no statistical evidence of an increasing airborne fraction but we do find statistical evidence of a decreasing sink rate. We infer that the efficiency of the sinks to absorb CO₂ from the atmosphere is decreasing at approximately 0.54% per year.

Copyright statement. TEXT

10 1 Introduction

A part of the anthropogenically released CO₂ emitted to the atmosphere flows to the oceans (the ocean sink) and the terrestrial biosphere (the land sink). Approximately 45% of released CO₂ stays in the atmosphere (the airborne fraction), while the two sinks take up approximately 24% and 31% of the CO₂, respectively. A key question is whether the airborne fraction is increasing or if it remains constant at around 45%. Closely related is the question whether the sinks will continue taking up CO₂ at the same rate (the sink rate) or if this rate is decreasing. The answers to these questions are important for our understanding of the global carbon cycle and consequently for policy makers and the public in general.

A series of papers argue that the airborne fraction of anthropogenically released CO₂ (mainly through fossil fuel emissions, cement production, and land-use change) is increasing (Canadell et al., 2007; Le Quéré et al., 2009; Raupach et al., 2008). Similarly, in Raupach et al. (2014) it is argued that, although the statistical evidence of an increasing airborne fraction is relatively weak, the evidence of a decreasing CO₂ sink rate is clearer. However, the methods in these studies have been



criticized in, for example, Knorr (2009), Gloor et al. (2010), and Ballantyne et al. (2015). Indeed, by considering a longer data set and incorporating uncertainties into the data, Knorr (2009) found that the conclusion of an increasing airborne fraction was not warranted. Similarly, Ballantyne et al. (2015) argues that errors in the data can lead to erroneous conclusions regarding possible trends in the airborne fraction and in the sink rate.

5 In this paper, we conduct a statistical analysis of the dynamics and interactions of anthropic emissions of CO₂ and its uptake in the atmosphere, the oceans, and the terrestrial biosphere. We study both the airborne fraction and the CO₂ sink rate. The statistical problem is cast in a *state space system*, which we argue is well designed for the problem at hand. The state space framework allows us to conduct statistical inference by taking explicit account of stochastic and deterministic trends in the data, transient shocks to the data (coming from, e.g., volcanic eruptions or strong El Niño events), and (potential) measurement
10 errors. The state space system allows for the simultaneous incorporation of multiple data sets for the same object, which can improve estimation and increase reliability of parameter estimates. By assuming a balanced carbon budget (Le Quéré et al., 2018), we obtain more than one data series of the same physical object of interest (e.g., the airborne fraction or the CO₂ sink rate). This seems particularly important in the context of the global carbon budget data considered here, which goes back only to 1959.

15 The paper is organized as follows. In Sect. 2 we state the fundamental equations of the global carbon budget, the airborne fraction of anthropogenically released CO₂, and the CO₂ sink rate, which will motivate the specification of the state space model. Sect. 3 introduces the state space models used in the paper. In Sect. 4 we conduct a trend analysis of the airborne fraction. In Sect. 5 we carry out the corresponding analysis of the CO₂ sink rate and in Sect. 6 of the land and ocean sink rates separately. Sect. 7 discusses the results and Sect. 8 concludes.

20 2 The global carbon budget

The so-called *carbon budget* is defined as

$$E_t^{ANT} = G_t + S_t^O + S_t^L, \quad (1)$$

where E_t^{ANT} is anthropogenically released CO₂ into the atmosphere, G_t is growth of atmospheric CO₂ concentration, S_t^O is the flux of CO₂ from the atmosphere to the oceans (the ocean sink), and S_t^L is the flux of CO₂ from the atmosphere to the
25 terrestrial biosphere (the land sink). We use the data set provided by The Global Carbon Project (Le Quéré et al., 2018).¹ The growth rate in atmospheric CO₂ data, G_t , is thus from Dlugokencky and Tans (2018), while the sink data, S_t^O and S_t^L , are averages over several independent model-based estimates, constructed as explained in Le Quéré et al. (2018). All data are given in gigatonnes of carbon (GtC) and are recorded at a yearly frequency, beginning in 1959 and ending in 2016, resulting in 58 observations for each quantity in (1).

30 The anthropogenic emissions of CO₂ are defined as

$$E_t^{ANT} = E_t^{FF} + E_t^{LUC},$$

¹The data are available at <http://www.globalcarbonproject.org/> and were downloaded on June 1st, 2018.



based where E_t^{FF} is emissions from fossil fuel burning, cement production, and gas flaring, while E_t^{LUC} is emissions from land-use change. The former data, E_t^{FF} , are from Boden et al. (2018), while the latter data, E_t^{LUC} , are averages over the model-based estimates of Hansis et al. (2015) and Houghton and Nassikas (2017), updated as in Le Quéré et al. (2018). The time series of concentrations (above preindustrial levels) of CO_2 in the atmosphere is constructed as

$$5 \quad C_t = 2.127 \cdot ([\text{CO}_2]_{1959} - [\text{CO}_2]_{1750}) + \sum_{\tau=1}^t G_{\tau},$$

where $[\text{CO}_2]_{1750} = 279$ ppmv (parts per million volume) and $[\text{CO}_2]_{1959} = 315.39$ ppmv are the concentrations of CO_2 in the atmosphere in 1750 and 1959, respectively; see Raupach et al. (2014). The number 2.127 is the conversion factor from ppmv to GtC.

In words, Eq. (1) states that emissions of CO_2 should equal the fluxes of CO_2 to the atmosphere, the ocean sink, and the land sink. The term G_t is a growth rate per unit time, and sometimes it is written in the continuous time version as

$$G_t = \frac{dC_t}{dt}.$$

While the carbon budget is in principle always balanced, in the sense that Eq. (1) always holds, this might not be the case when inserting actual data for emissions and sinks, due to measurement errors in the data. The residual term is referred to as the *budget imbalance* by Le Quéré et al. (2018) and is denoted by B_t^{IM} . Therefore, when considering actual data, the carbon budget is defined as

$$15 \quad E_t^{ANT} = G_t + S_t^O + S_t^L + B_t^{IM}. \quad (2)$$

We follow Raupach et al. (2014) and define the airborne fraction

$$AF_t = \frac{G_t}{E_t^{ANT}}$$

and the sink fraction

$$20 \quad SF_t = \frac{S_t^O + S_t^L}{E_t^{ANT}} = 1 - AF_t,$$

where the second equality assumes that B_t^{IM} is equal to zero. These fractions are for the anthropogenically released CO_2 that stays in the atmosphere (AF_t) and in the combined sink of ocean plus land (SF_t). One can also consider the ocean and land sinks separately and define the ocean and land fractions as

$$OF_t = \frac{S_t^O}{E_t^{ANT}}, \quad LF_t = \frac{S_t^L}{E_t^{ANT}},$$

25 respectively, with $SF_t = OF_t + LF_t$.

Following Raupach (2013) and Raupach et al. (2014), we further consider the CO_2 sink rate which is defined at time t by

$$k_{S,t} = \frac{S_t^O + S_t^L}{C_t}, \quad (3)$$



which is the flux of CO₂ from the atmosphere into the sinks (ocean plus land), normalized by the amount of CO₂ (above preindustrial levels) currently in the atmosphere. Using a simplifying linear specification, Gloor et al. (2010) interprets the variable $k_{S,t}$ as a “sink efficiency”.

From the global carbon budget (1), it follows that the sink efficiency $k_{S,t}$ can alternatively be written as

$$5 \quad k_{S,t} = \frac{E_t^{ANT} - G_t}{C_t}. \quad (4)$$

We can also consider the individual components of the sink rate for ocean and land which are given by

$$k_{O,t} = \frac{S_t^O}{C_t}, \quad k_{L,t} = \frac{S_t^L}{C_t}, \quad (5)$$

respectively, with $k_{S,t} = k_{O,t} + k_{L,t}$.

3 Trend model specification

10 In this section, we consider several models for the data generating process behind observations of the objects of interest defined in Sect. 2. Common to all models is that they can be cast in a state space system of the form:

$$\begin{aligned} y_t &= Ax_t + \xi_t, \\ x_{t+1} &= Bx_t + \kappa_t, \end{aligned} \quad t = 1, \dots, n, \quad (6)$$

where y_t is a vector of observations at time $t = 1, \dots, n$ with time series length n , the system matrices A and B have appropriate dimensions, the vector x_t is usually referred to as the state vector which can include deterministic and stochastic trends, and the error terms ξ_t and κ_t are both independent and identically distributed (iid) random vectors of appropriate dimension and with mean zero. For example, when we need to model the airborne fraction alone, we have $y_t = AF_t$ and the state space system represents a univariate dynamic model for the airborne fraction. When modelling the ocean and land fractions jointly, we have $y_t = (OF_t, LF_t)'$ and the state space system is for a bivariate dynamic model. For given matrices A and B , and under the assumption of mutually and serially uncorrelated Gaussian errors ξ_t and κ_t (with their respective variance matrices Σ_ξ and Σ_κ), the state space system is a linear Gaussian model. In such regular cases, an analytic formulation for the likelihood function is available and relies on the prediction error decomposition. Hence the parameters (variances and possibly covariances in Σ_ξ and Σ_κ) can be estimated by the maximum likelihood method. It requires the numerical optimization of the log-likelihood function that is evaluated via the Kalman filter. The smooth estimate of the state process x_t can also be obtained by means of the Kalman filter together with a smoothing algorithm. The extracted state is effectively the conditional mean $\mathbb{E}(x_t | y_1, \dots, y_n; A, B, \Sigma_\xi, \Sigma_\kappa)$, for $t = 1, \dots, n$. Details of the state space approach to time series modeling, including the statistical treatment of the initial state x_1 , are given by Durbin and Koopman (2012) where both signal extraction and maximum likelihood estimation are discussed.



Our baseline model is the local linear trend (LLT) model with a fixed and unknown growth (or slope) coefficient.² For a univariate time series y_t , we treat the underlying trend T_t as a stochastic process given by

$$T_{t+1} = T_t + \beta + \eta_t, \quad (7)$$

where $\beta \in \mathbb{R}$ is a fixed and unknown coefficient and η_t is an iid Gaussian random variable with mean zero and variance σ_η^2 .

5 The solution to the difference equation (7) is given as

$$T_{t+1} = T_1 + t\beta + \sum_{i=0}^{t-1} \eta_{t-i}, \quad t = 1, 2, \dots, n-1,$$

where T_1 can be treated as a fixed unknown coefficient (intercept or constant) or as a random variable. It shows that the trend component is made up of the starting value T_1 , a deterministic linear term with slope β , and the random walk component $\sum_{i=0}^{t-1} \eta_{t-i}$. In this way, T_t can be interpreted as a long-term trend in the time series and β as the slope of the deterministic part

10 of the trend. The observation equation for y_t is given by

$$y_t = T_t + \epsilon_t, \quad (8)$$

where T_t is given by (7) and ϵ_t captures deviations of the observed time series from the unobserved trend component. The deviations ϵ_t can be viewed as (i) actual (transient) disturbances of the physical systems arising from, for example, volcanic eruptions and El Niño events, and/or (ii) measurement errors arising from the way the data are collected.³ The random variable

15 ϵ_t is assumed to be iid Gaussian with mean zero and variance σ_ϵ^2 .

The local linear trend model can be cast in the state space system (6) where vectors and matrices are defined as

$$x_t = \begin{pmatrix} T_t \\ \beta \end{pmatrix}, \quad A = \begin{bmatrix} 1 & 0 \end{bmatrix}, \quad B = \begin{bmatrix} 1 & 1 \\ 0 & 1 \end{bmatrix}, \quad \xi_t = \epsilon_t, \quad \kappa_t = \begin{pmatrix} \eta_t \\ 0 \end{pmatrix},$$

for $t = 1, \dots, n$. The state vector x_t consists of the two variables of interest: stochastic trend variable T_t and deterministic slope variable β . The state space methods as discussed above can treat such mixed compositions of the state vector. We have
 20 illustrated how the state space system can be used for a univariate time series. In the next sections, we also consider trend analyses based on multivariate time series models.

4 Trend analysis of the airborne fraction

When we assume that the carbon budget is balanced, see the discussion in Sect. 2, for all time periods $t = 1, \dots, n$, we can measure the airborne fraction AF_t in two alternative ways:

$$25 \quad AF_t^{(1)} = \frac{G_t^{ATM}}{E_t^{ANT}}, \quad AF_t^{(2)} = 1 - SF_t = 1 - \frac{S_t^O + S_t^L}{E_t^{ANT}}. \quad (9)$$

²We also considered a time-varying slope but found no evidence supporting this generalization in either the airborne fraction or the sink rate.

³See Ballantyne et al. (2015) for the importance of accounting for measurement errors in the data.



Although these two quantities measure the same underlying object (the airborne fraction AF_t), they may differ when we consider the actual data; see also Eq. (2). We consider our baseline local linear trend model of Sect. 3 for each of the objects, that is

$$y_t = AF_t^{(i)} = T_t^{(i)} + \epsilon_t^{(i)},$$

- 5 for $i = 1, 2$, where the trend $T_t^{(i)}$ is specified in (7) and with error $\epsilon_t^{(i)}$. Table 1 reports the output of the estimation, using the state space system and the Kalman filter. The first part of Table 1 presents estimates of the standard deviations of the error terms ϵ and η , as well as the estimate of the slope parameter β , including the estimated standard deviation of $\hat{\beta}$ and the resulting t -statistic, $t\text{-stat} = \frac{\hat{\beta}}{\text{s.d.}(\hat{\beta})}$. Based on these estimation results, we can formally test hypotheses of the type

$$H_0 : \beta = 0 \quad \text{against} \quad H_1 : \beta \neq 0, \tag{10}$$

- 10 or, more relevantly,

$$H_0 : \beta = 0 \quad \text{against} \quad H_1 : \beta > 0. \tag{11}$$

By using the normal approximation to the t -distribution and for a 95% confidence level, the critical value for the test (10) is 1.96, and for (11) it is 1.645. In case of the airborne fraction, we are interested in testing (11). It is evident from Table 1 that we cannot reject H_0 in this case. In other words, although the estimate $\hat{\beta}$ is positive, we cannot conclude, statistically at 95%
 15 confidence, that the airborne fraction is increasing over time.

Table 1 also contains diagnostic statistics for the standardized prediction residual u_t based on $y_t - \mathbb{E}(y_t | y_1, \dots, y_{t-1}; A, B, \Sigma_\xi, \Sigma_\kappa)$, for $t = 1, \dots, n$, and where Σ_ξ and Σ_κ are replaced by their respective maximum likelihood estimates. Under the assumption that the local linear trend model is correctly specified for the time series y_t , the residuals u_t are Gaussian iid; see (Durbin and Koopman, 2012, p.38). To verify these properties of u_t empirically, we consider two residual diagnostic statistics: the
 20 normality test statistic N of Jarque and Bera (1987) and the serial correlation test statistic DW of Durbin and Watson (1971). As a goodness-of-fit statistic, we consider the R_d^2 which is a relative measure of model fit against a random walk model. The statistic is defined in a similar way as the standard regression fit measure R^2 , we have

$$R_d^2 = 1 - \frac{\sum_{t=2}^n u_t^2}{\sum_{t=2}^n [(y_t - y_{t-1}) - m]^2}, \quad m = (n-1)^{-1} \sum_{t=2}^n (y_t - y_{t-1}).$$

The reported diagnostic statistics and goodness-of-fit in Table 1 are satisfactory for the time series $AF_t^{(1)}$ and $AF_t^{(2)}$. We may
 25 conclude from these results that the local linear trend model (7)-(8) provides an adequate description of the dynamic features in the time series.

The state space system allows both measures for the airborne fraction, $AF_t^{(1)}$ and $AF_t^{(2)}$, to be included in a single model with the purpose to improve the quality of the trend estimation and inference. We begin with an “uninformed” system using



Table 1. Univariate analysis of the airborne fraction

	Parameter estimates					Diagnostics		
	$\hat{\sigma}_\epsilon$	$\hat{\sigma}_\eta$	$\hat{\beta}$	s.e.($\hat{\beta}$)	t -stat($\hat{\beta}$)	N	R_d^2	DW
$AF_t^{(1)}$	0.1357	0.0101	0.00109	0.00179	0.60934	0.274	0.442	1.829
$AF_t^{(2)}$	0.1353	0.0122	0.00049	0.00203	0.24246	2.324	0.489	1.9905

We report parameter estimates for the standard deviations σ_ϵ and σ_η , and slope coefficient β together with its standard error (s.e.) and t -statistic (t -stat). We further report the normality (N) test, the goodness-of-fit statistic R_d^2 and the Durbin-Watson (DW) test statistic for serial correlation; all computed for the standardized prediction errors u_t which are obtained from the Kalman filter. The normality test N is the χ^2 distributed, with 2 degrees of freedom, statistic of Jarque and Bera (1987) with its 95% critical value of 5.99; the statistic relies on the sample estimates of skewness and kurtosis of u_t . The goodness-of-fit statistic R_d^2 is defined as $1 - ESS/DSS$ where $ESS = \sum_{t=2}^n u_t^2$ and $DSS = \sum_{t=2}^n [(y_t - y_{t-1}) - m]^2$ with $m = (n-2)^{-1} \sum_{t=2}^n (y_t - y_{t-1})$. The Durbin-Watson DW test statistic is developed by Durbin and Watson (1971), where also its critical values are tabulated. If $DW = 2$ the sequence u_t is serially uncorrelated; if $DW < 2$ there is evidence that the errors u_t are positively autocorrelated; if $DW > 2$ there is evidence that the errors u_t are negatively autocorrelated.

two different trend components, $T_t^{(1)}$ and $T_t^{(2)}$, both specified as (7), for the two time series, we have

$$y_t = \begin{bmatrix} AF_t^{(1)} \\ AF_t^{(2)} \end{bmatrix} = \begin{bmatrix} G_t^{ATM}/E_t^{ANT} \\ 1 - (S_t^{OCEAN} + S_t^{LAND})/E_t^{ANT} \end{bmatrix} = \begin{bmatrix} T_t^{(1)} \\ T_t^{(2)} \end{bmatrix} + \begin{bmatrix} \epsilon_t^{(1)} \\ \epsilon_t^{(2)} \end{bmatrix}, \quad (12)$$

where the error terms $\epsilon_t^{(i)}$, for $i = 1, 2$, are correlated and its correlation coefficient can be estimated by the method of maximum likelihood together with the other parameters. The estimation results for this model are presented in Panel A of Table 2. The main difference to Table 1 is the inclusion of the estimated correlation matrix for $(\epsilon_t^{(1)}, \epsilon_t^{(2)})$. The diagnostic test statistics are reasonable. In comparison with the univariate analysis, the goodness-of-fit values for R_d^2 are slightly higher for the multivariate model. Hence we trust the model to be a good representation of the data. Furthermore, the slope is estimated to be positive in both cases (that is $\hat{\beta} > 0$), indicating an increasing airborne fraction. However, when testing the null hypothesis given in (11), we cannot reject the hypothesis that the slopes are zero.

10

Since the two quantities in (9) are measuring the same object, the airborne fraction, we now force the state space system to recognize that these data are driven by the same underlying common trend, T_t^A say, but with possibly different error terms $\epsilon_t^{(1)}$ and $\epsilon_t^{(2)}$. In other words, we consider

$$y_t = \begin{bmatrix} AF_t^{(1)} \\ AF_t^{(2)} \end{bmatrix} = \begin{bmatrix} G_t^{ATM}/E_t^{ANT} \\ 1 - (S_t^{OCEAN} + S_t^{LAND})/E_t^{ANT} \end{bmatrix} = \begin{bmatrix} T_t^A \\ T_t^A \end{bmatrix} + \begin{bmatrix} \epsilon_t^{(1)} \\ \epsilon_t^{(2)} \end{bmatrix}. \quad (13)$$

15 The output of the estimation of this system is shown in Panel B of Table 2; the estimated common trend and the data are plotted in Fig. 1. A slight deterioration of the diagnostic statistics is to be expected when introducing a common trend into the system, but the diagnostic statistics are still such that we can accept (13) as a plausible model. For the estimate of the slope $\hat{\beta}$, we find a larger t -statistic in absolute value than in the uninformed model, indicating the restriction to the common trend



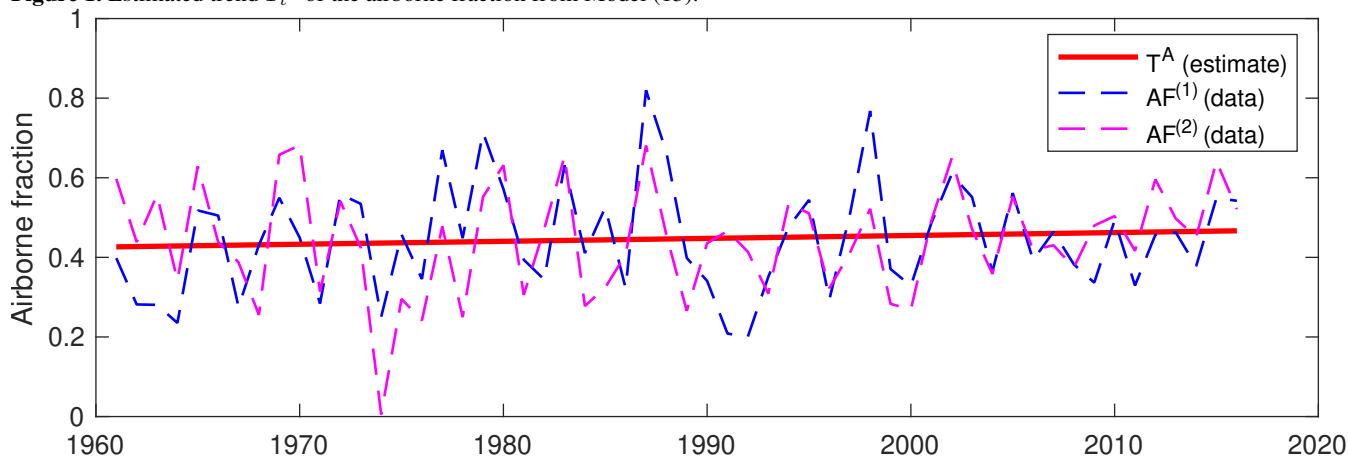
Table 2. Multivariate analysis of the airborne fraction

	Parameter estimates					Correlation matrix (ϵ)		Diagnostics		
Panel A: Two individual trends as in Eq. (12).										
	$\hat{\sigma}_\epsilon$	$\hat{\sigma}_\eta$	$\hat{\beta}$	s.e.($\hat{\beta}$)	t-stat($\hat{\beta}$)	$AF^{(1)}$	$AF^{(2)}$	N	R_d^2	DW
$AF^{(1)}$	0.1268	0.0333	0.00146	0.00459	0.31797	1.0000	0.7612	0.603	0.484	2.0152
$AF^{(2)}$	0.1307	0.0274	0.00010	0.00383	0.02629	0.7612	1.0000	1.469	0.525	2.0853
Panel B: One common trend as in Eq. (13).										
	$\hat{\sigma}_\epsilon$	$\hat{\sigma}_\eta$	$\hat{\beta}$	s.e.($\hat{\beta}$)	t-stat($\hat{\beta}$)	$AF^{(1)}$	$AF^{(2)}$	N	R_d^2	DW
$AF^{(1)}$	0.1370	7.2e-09	0.00073	0.00095	0.77258	1.0000	0.5518	0.245	0.470	1.8722
$AF^{(2)}$	0.1375	–	–	–	–	0.5518	1.0000	2.573	0.516	1.9820

We report parameter estimates for the standard deviations $\sigma_\epsilon^{(i)}$ and $\sigma_\eta^{(i)}$, for $i = 1, 2$, correlation matrix for ϵ_t , and slope coefficient β together with its standard error (s.e.) and t -statistic (t -stat). We further report the normality (N) test, the goodness-of-fit statistic R_D^2 and the Durbin-Watson (DW) test statistic for serial correlation; for details see Table 1. In Panel B, the trend coefficients (σ_η and β) for $AF^{(2)}$ are the same as for $AF^{(1)}$ given the construction of model (13).

increases the precision of the estimates. An explanation of this finding is that the informed system in effect has used twice as many observations for estimating the trend, when compared to the uninformed system. The hypothesis test (11) reveals that the estimate of the slope parameter, although again positive, is still not statistically different from zero.

Figure 1. Estimated trend T_t^A of the airborne fraction from Model (13).



5 Trend analysis of the CO₂ sink rate

- 5 In this section, we analyse the CO₂ sink rate in the same way as the airborne fraction above. The definition of the sink rate is given in Eq. (3). The assumption of a balanced carbon budget provides the alternative definition (4). As a result we can now



define two alternative versions of the sink rate:

$$k_{S,t}^{(1)} = \frac{S_t^O + S_t^L}{C_t}, \quad k_{S,t}^{(2)} = \frac{E_t^{ANT} - G_t}{C_t}.$$

Our basic (univariate) local linear trend model for each of these objects is then given by

$$y_t = k_{S,t}^{(i)} = T_t^{(i)} + \epsilon_t^{(i)},$$

- 5 for $i = 1, 2$, where $T_t^{(i)}$ is specified as in (7). When the model is cast in the state space system, the parameters can be estimated for each of the data series individually. The estimation results are presented in Table 3. The diagnostic statistics are again satisfactory. Although we do have negative estimates of the slopes, we cannot reject the null hypothesis of $\beta = 0$. We still consider a one-sided test as in (11) but now the relevant alternative hypothesis is $H_1 : \beta < 0$.

Table 3. Univariate analysis of the CO₂ sink rate

	Parameter estimates					Diagnostics		
	$\hat{\sigma}_\epsilon$	$\hat{\sigma}_\eta$	$\hat{\beta}$	s.e.($\hat{\beta}$)	t -stat($\hat{\beta}$)	N	R_d^2	DW
$k_S^{(1)}$	0.0066	8.8077e-04	-0.00010	0.00013	-0.76117	4.880	0.464	1.968
$k_S^{(2)}$	0.0063	6.3982e-04	-0.00015	0.00010	-1.43179	0.967	0.442	1.875

We report parameter estimates for the standard deviations σ_ϵ and σ_η , and slope coefficient β together with its standard error (s.e.) and t -statistic (t -stat). We further report the normality (N) test, the goodness-of-fit statistic R_D^2 and the Durbin-Watson (DW) test statistic for serial correlation; all computed for the standardized prediction errors u_t which are obtained from the Kalman filter; for details see Table 1.

- 10 Similar to the airborne fraction above, these data can be put in a joint “uninformed” system with two different trend components, and we have

$$y_t = \begin{bmatrix} k_{S,t}^{(1)} \\ k_{S,t}^{(2)} \end{bmatrix} = \begin{bmatrix} (S_t^O + S_t^L)/C_t \\ (E_t^{ANT} - G_t)/C_t \end{bmatrix} = \begin{bmatrix} T_t^{(1)} \\ T_t^{(2)} \end{bmatrix} + \begin{bmatrix} \epsilon_t^{(1)} \\ \epsilon_t^{(2)} \end{bmatrix}, \quad (14)$$

which can be compared with model (12). The estimation results for this model are reported in Panel A of Table 4. Although the slope estimates are negative, they are not significantly negative.

15

Finally, we consider the state space system that imposes a common trend for both time series, T_t^S say, that is

$$y_t = \begin{bmatrix} k_{S,t}^{(1)} \\ k_{S,t}^{(2)} \end{bmatrix} = \begin{bmatrix} (S_t^O + S_t^L)/C_t \\ (E_t^{ANT} - G_t)/C_t \end{bmatrix} = \begin{bmatrix} T_t^S \\ T_t^S \end{bmatrix} + \begin{bmatrix} \epsilon_t^{(1)} \\ \epsilon_t^{(2)} \end{bmatrix}, \quad (15)$$

which can be compared with model (13). The estimation results are presented in Panel B of Table 4. Similar to our analysis of the airborne fraction in the previous section, the diagnostic statistics are somewhat worse for our less flexible system with



Table 4. Multivariate analysis of the CO₂ sink rate

		Parameter estimates					Correlation matrix (ϵ)		Diagnostics		
Panel A: Two individual trends as in Eq. (14).											
		$\hat{\sigma}_\epsilon$	$\hat{\sigma}_\eta$	$\hat{\beta}$	s.e.($\hat{\beta}$)	t -stat($\hat{\beta}$)	$AF^{(1)}$	$AF^{(2)}$	N	R_d^2	DW
$k_S^{(1)}$		0.0064	0.0015	-0.00010	0.00020	-0.49406	1.0000	0.7733	3.348	0.511	2.0233
$k_S^{(2)}$		0.0060	0.0014	-0.00017	0.00020	-0.86071	0.7733	1.0000	1.365	0.488	2.0185
Panel B: One common trend as in Eq. (15).											
		$\hat{\sigma}_\epsilon$	$\hat{\sigma}_\eta$	$\hat{\beta}$	s.d.($\hat{\beta}$)	t -stat($\hat{\beta}$)	$k_S^{(1)}$	$k_S^{(2)}$	N	R_d^2	DW
$k_S^{(1)}$		0.0068	4.1762e-09	-0.00014	0.00005	-2.99145	1.0000	0.5621	4.012	0.499	2.0276
$k_S^{(2)}$		0.0065	–	–	–	–	0.5621	1.0000	0.090	0.474	1.7967

We report parameter estimates for the standard deviations $\sigma_\epsilon^{(i)}$ and $\sigma_\eta^{(i)}$, for $i = 1, 2$, correlation matrix for ϵ_t , and slope coefficient β together with its standard error (s.e.) and t -statistic (t -stat). We further report the normality (N) test, the goodness-of-fit statistic R_D^2 and the Durbin-Watson (DW) test statistic for serial correlation; for details see Table 1. In Panel B, the trend coefficients (σ_η and β) for $k_S^{(2)}$ are the same as for $k_S^{(1)}$ given the construction of model (15).

a common trend. However, the diagnostics are still satisfactory while the goodness-of-fit statistics have improved overall. Our estimate of the slope is

$$\hat{\beta} = -0.00014,$$

and this estimate is statistically significant: we reject the hypothesis $H_0 : \beta = 0$ in favor of $H_1 : \beta < 0$ at a 95% confidence level. The mean of the sink rate (calculated using either data set $k_S^{(1)}$ or $k_S^{(2)}$) is 0.0258. It follows that we estimate the sink rate to be decreasing with approximately $0.00014/0.0258 = 0.54\%$ every year. The estimated trend and the data are plotted in Fig. 2.

The state space system is also well-suited for forecasting; see Durbin and Koopman (2012). The output of the forecasting exercise for the sink rate is presented in Fig. 3 where we forecast the sink rate 25 years ahead in time. The decreasing nature of the forecasts is clearly visible.

6 Trend analysis of the ocean and land sink rates

We may conclude from the analysis in the previous section that the combined (land plus ocean) sink rate appears to be decreasing. To verify this finding in more detail, we can consider the two sink variables separately. The analysis can be done simultaneously based on the model

$$y_t = \begin{bmatrix} k_{O,t} \\ k_{L,t} \end{bmatrix} = \begin{bmatrix} S_t^O / C_t \\ S_t^L / C_t \end{bmatrix} = \begin{bmatrix} T_t^O \\ T_t^L \end{bmatrix} + \begin{bmatrix} \epsilon_t^{(1)} \\ \epsilon_t^{(2)} \end{bmatrix}, \quad (16)$$



Figure 2. Estimated trend T_t^S of the CO₂ sink rate from Model (15).

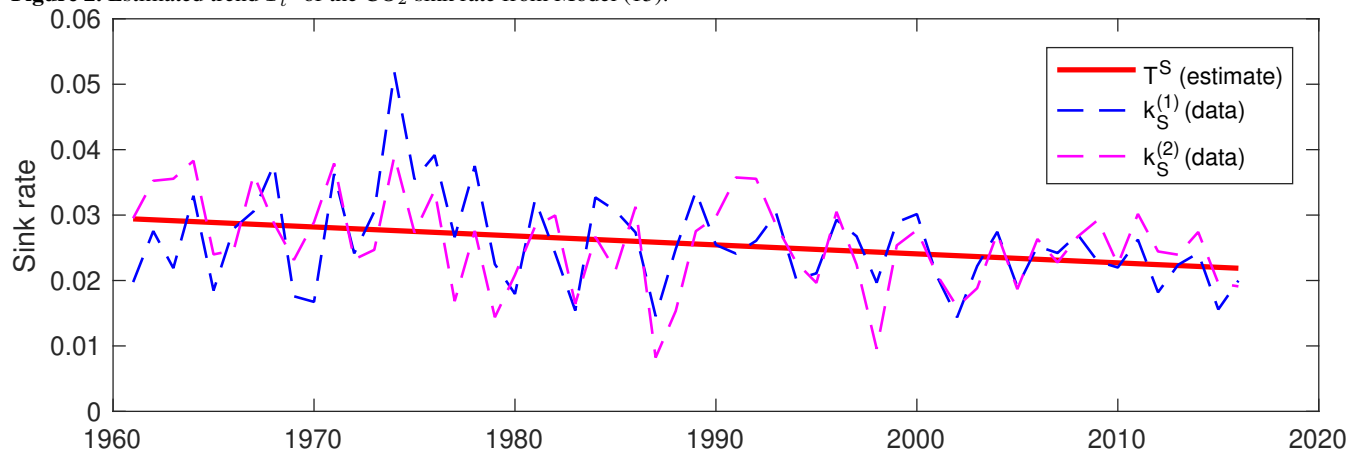


Figure 3. Forecasting the CO₂ sink rate based on Model (15).

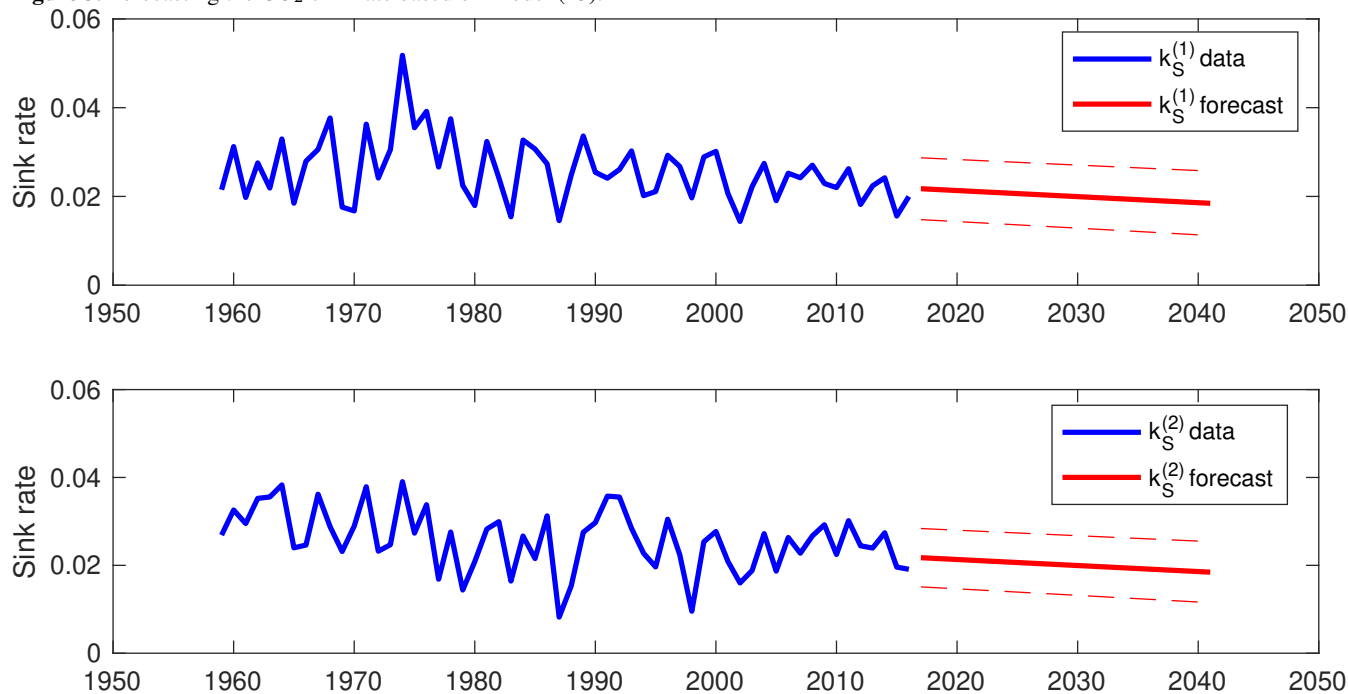


Figure 3. The blue solid line represents the data, while the red solid line represents the point forecasts from the Kalman filter with the unknown parameters estimated by maximum likelihood. The dashed red lines are 68.3% confidence bands (± 1 standard deviation) for the forecasts.



where the time series $k_{O,t}$ and $k_{L,t}$ are defined in (5) while the trend variables T_t^O and T_t^L are specified as in (7). To inform the state space system of the structure of the carbon budget, we consider the model equations

$$y_t = \begin{bmatrix} k_{O,t} \\ k_{L,t} \\ k_{S,t} \end{bmatrix} = \begin{bmatrix} S_t^O/C_t \\ S_t^L/C_t \\ (E_t^{ANT} - G_t)/C_t \end{bmatrix} = \begin{bmatrix} T_t^O \\ T_t^L \\ T_t^O + T_t^L \end{bmatrix} + \begin{bmatrix} \epsilon_t^{(1)} \\ \epsilon_t^{(2)} \\ \epsilon_t^{(3)} \end{bmatrix}. \quad (17)$$

Also this trivariate model equation can be cast in the state space system (6). The model specification has two independent trend processes of the form (7) for land and ocean sinks. The $k_{S,t}$ time series of combined ocean and land sinks must therefore feature the sum of the two trend processes for the individual sinks as its trend process.

The estimation results for these two model specifications are presented in Table 5. The residual diagnostic statistics N and DW are satisfactory, but we are particularly interested in the estimates of the slope parameters. It seems that most of the decrease in the sink rate can be attributed to the land sink. The slope estimates of the trend driving the ocean sink rate are very close to zero and not statistically different from zero. On the other hand, the slope estimates of the trend driving the land sink rate are negative for both specifications. In the first model (16), we can reject the hypothesis that the slope of the trend driving the land sink rate is zero, in favor of the one-sided alternative $H_1 : \beta < 0$ at a 95% confidence level. For the more informed model specification (17), the estimation results are reported in Panel B of Table 5. We learn from this analysis that the estimate of the slope parameter from the land sink rate is equal to the estimate of the slope parameter from the combined sink rate as we have found it in Sect. 5, that is $\hat{\beta} = -0.00014$. In other words, it appears that the slope in the land sink rate explains all of the slope in the combined sink rate studied in the previous section.

In summary, the statistical evidence presented for the trivariate model is not as strong as we have presented for the model of the combined sink rate in the previous section. For instance, if we would have conducted the two-sided test (10), as opposed to the one-sided test in (11), on the basis of model specification (16), with the results presented in Panel A of Table 5, we could not have rejected $H_0 : \beta = 0$ in favor of $H_1 : \beta \neq 0$. Nevertheless, the findings of this section provide some evidence that the decrease in the sink rate, as found in Sect. 5 above, is mainly driven by a decrease in the land sink rate.

7 Discussion

Previous studies of the airborne fraction and the CO₂ sink rate have focused on detecting a single linear and deterministic trend in the data of the form $a_0 + a_1 t$, where a_0, a_1 are constants (Canadell et al., 2007; Le Quéré et al., 2009; Knorr, 2009; Raupach et al., 2008, 2014). However, possible statistical difficulties in such analyses have been pointed out in Knorr (2009). For instance, a linear regression analysis can yield invalid inference if the data are non-stationary, e.g., if they contain trends (Granger and Newbold, 1974). The approach of this paper is to consider the data in a state space system. In this way, non-stationary components are explicitly modelled as unobserved trend components and inference is valid (e.g., Durbin and Koopman, 2012). Furthermore, the trend specification of the state space system allows for both deterministic and stochastic trend components.



Table 5. Analysis of ocean and land sink rates

Panel A: Two trends, two observation series as in Eq. (16).											
	Parameter estimates					Correlation matrix (ϵ)		Diagnostics			
	$\hat{\sigma}_\epsilon$	$\hat{\sigma}_\eta$	$\hat{\beta}$	s.d.($\hat{\beta}$)	t-stat($\hat{\beta}$)	$k_{O,t}$	$k_{L,t}$	N	R_d^2	DW	
$k_{O,t}$	0.0001	0.00081	0.00001	0.00011	0.057	1.00	-1.00	4.839	0.0343	1.847	
$k_{L,t}$	0.0067	0.00015	-0.00010	0.00006	-1.728	-1.00	1.00	5.332	0.513	1.908	
Panel B: Two trends, three observation series as in Eq. (17).											
	$\hat{\sigma}_\epsilon$	$\hat{\sigma}_\eta$	$\hat{\beta}$	s.d.($\hat{\beta}$)	t-stat($\hat{\beta}$)	$k_{O,t}$	$k_{L,t}$	$k_{S,t}$	N	R_d^2	DW
	$k_{O,t}$	0.0001	0.00081	0.00000	0.0001	0.0422	1.00	-0.122	-0.884	4.839	0.0343
$k_{L,t}$	0.0068	0.00068	-0.00014	0.0001	-1.352	-0.122	1.00	0.572	4.054	0.494	1.989
$k_{S,t}$	0.0065	-	-	-	-	-0.884	0.572	1.00	1.114	0.477	1.801

We report parameter estimates for standard deviations $\sigma_\epsilon^{(i)}$ and $\sigma_\eta^{(i)}$, for $i = 1, 2, 3$, correlation matrix for ϵ_t , and slope coefficient β together with its standard error (s.e.) and t -statistic (t -stat). We further report the normality (N) test, the goodness-of-fit statistic R_D^2 and the Durbin-Watson (DW) test statistic for serial correlation; for details see Table 1. In Panel B, we have two trends and two sets of trend coefficients (σ_η and β) for $k_{O,t}$ and $k_{L,t}$, the trend for $k_{S,t}$ is a combination of the two, given the construction of model (17).

Further, several studies have highlighted the need for accounting for noise in measurements of climate-related data (Knorr, 2009; Ballantyne et al., 2015). The state space approach explicitly incorporates such noise in the framework as well. Ballantyne et al. (2015) argue that errors in E_t^{ANT} might be autocorrelated. As shown in Tables 1 through 5, the diagnostic statistics do not indicate that autocorrelated errors pose a serious problem. Nevertheless, the state space framework can incorporate autocorrelated errors in the measurement equation.

This paper considers data recorded at a yearly frequency, while many of the previous studies of the airborne fraction and the sink rate use monthly data. The advantage of using monthly data is obvious: more observations. However, there are also some downsides. For instance, while the CO_2 concentration C_t (and therefore also the growth rate G_t) are recorded every month, these data contain a strong seasonal component induced by the photosynthesis/respiration cycle of terrestrial vegetation. This seasonality needs to be accounted for in some way; for instance, Raupach et al. (2014) smooth the data using a 15-month running mean. Conversely, some of the other data are recorded only yearly; for instance, the emissions data available to us, E_t^{ANT} , are reported at a yearly frequency. In this case Raupach et al. (2014) use linear interpolation to get monthly estimates of emissions. Such transformations of the data, i.e., smoothing or interpolation, might introduce new and complicated errors into the transformed data, possibly invalidating the analyses. For these reasons, we prefer to work with yearly data.

Why do we find statistical evidence of a decreasing CO_2 sink rate but no evidence of an increasing airborne fraction when these two quantities are closely linked and the data going into the analyses are the same? It was noted in Gloor et al. (2010) that the airborne fraction and the sink rate are actually not as closely linked as they seem *prima facie*. In particular, an increasing airborne fraction does not necessarily imply a decreasing sink rate (Gloor et al., 2010, Section 8). Secondly, we believe that the way the two quantities are defined makes the sink rate an easier object to study statistically. The idea of an airborne fraction (and a sink fraction) appears to be a long-term quantity: the airborne fraction should represent the amount of anthropogenically released CO_2 that eventually stays in the atmosphere, after other fluxes have been taking into account. However, the ratio of the



concurrent fluxes, i.e., G_t/E_t^{ANT} , is likely a very noisy measurement of this object. Also, as we saw above, it is reasonable to think that sink fluxes, and therefore indirectly G_t , will depend on the *level* of CO₂ in the atmosphere (i.e., $C_t = \sum G_t$), which is not captured by the concurrent ratio G_t/E_t^{ANT} . When studying the airborne fraction, it would perhaps be more reasonable to study an object taking this cumulative nature into account, e.g. $\sum G_t / \sum E_t^{ANT} = C_t / \sum E_t^{ANT}$. However, cumulative statistics of this type would present other difficulties. The dominance of the long-term history may mask sudden changes, for example. These difficulties are even more pronounced when studying the sink fractions SF, OF, and LF: observations such as S_t^O/E_t^{ANT} are very noisy and since, as just discussed, S_t actually depends on C_t and generally not directly on E_t^{ANT} , this makes it difficult to interpret the results directly. In contrast, the sink rate S_t/C_t , as a flow-to-stock ratio, is immediately compatible with the underlying theory, at least as long as the linear approximation of Gloor et al. (2010) is adequate.

10 In our “informed” models with a single trend object for two alternative time series, the extracted trends are practically deterministic, that is, the estimates of σ_{Slp} in Panel B of Tables 2 and 4 are near zero, cf. also Fig. 1 and 2. It is important to stress that our modeling framework for the trend component, as specified in (7), allows for the trend to vary stochastically over time. However, we have not found strong evidence for a stochastic trend in our analyses. In contrast, in some of the univariate models, cf. Table 1, Panel A of Table 2, and Panel A of Table 4, we estimate $\hat{\sigma}_{Slp} > 0$ and, thus, in these cases, we find evidence

15 of the trend component varying in time. This variability disappears, however, once we impose a common trend in the models. In other words, there is evidence that a simple deterministic trend fits the data well (both the airborne fraction and the sink rate), and therefore that allowing for time-variation in the trend is redundant.

8 Conclusions

We have argued that the state space system can be a useful approach to analyze possible trends in the airborne fraction of anthropogenically released CO₂ and in the CO₂ sink rate. We have shown that deterministic and stochastic trend processes can be explicitly and jointly incorporated as unobserved components, allowing for a valid inference, even when the observed time series are non-stationary. The state space framework also allows for the incorporation of multiple data sets for the same object, which can increase reliability of the resulting estimates.

We estimate a positive, yet statistically insignificant, slope in the data for the airborne fraction. The sink rate exhibits some evidence of a decreasing trend. Using two alternative time series as data and imposing a common trend component for both, we obtain a significantly negative deterministic trend slope in the sink rate.

Our analyses support the conclusions as set out by Raupach et al. (2014): the rate at which the combined (ocean plus land) sink takes up CO₂ from the atmosphere seems to be decreasing. The best estimate resulting from our state space model is that the CO₂ sink rate, and therefore the efficiency with which the combined land and ocean sink is absorbing carbon from the atmosphere, is decreasing with 0.54% per year. We do not find evidence of this rate itself changing over time.

Finally, there is tentative evidence that the decrease in the sink rate is mainly driven by a weakening uptake in the land sink. The statistical evidence for this is not strong, however, and we suggest that additional research must be conducted to further investigate this question.



Author contributions. All authors contributed equally to the paper.

Competing interests. No competing interests are present.

Acknowledgements. We would like to thank Corinne Le Quéré for permission to use the data set of Le Quéré et al. (2018), as well as for useful comments on the manuscript. MB and EH acknowledge financial support from the Independent Research Fund Denmark for the
5 project Econometric Modeling of Climate Change.



References

- Ballantyne, A. P., Andres, R., Houghton, R., Stocker, B. D., Wanninkhof, R., Anderegg, W., Cooper, L. A., DeGrandpre, M., Tans, P. P., Miller, J. B., Alden, C., and White, J. W. C.: Audit of the global carbon budget: estimate errors and their impact on uptake uncertainty, *Biogeosciences*, 12, 2565–2584, <https://doi.org/10.5194/bg-12-2565-2015>, <https://www.biogeosciences.net/12/2565/2015/>, 2015.
- 5 Boden, T. A., Marland, G., and Andres, R. J.: Global, Regional, and National Fossil-Fuel CO₂ Emissions, oak Ridge National Laboratory, U.S. Department of Energy, Oak Ridge, Tenn., USA, available at: http://cdiac.ornl.gov/trends/emis/overview_2014.html, last access: 28 June 2017, 2018.
- Canadell, J. G., Le Quééré, C., Raupach, M. R., Field, C. B., Buitenhuis, E. T., Ciais, P., Conway, T. J., Gillett, N. P., Houghton, R. A., and Marland, G.: Contributions to accelerating atmospheric CO₂ growth from economic activity, carbon intensity, and efficiency of
10 natural sinks, *Proceedings of the National Academy of Sciences*, 104, 18 866–18 870, <https://doi.org/10.1073/pnas.0702737104>, <http://www.pnas.org/content/104/47/18866>, 2007.
- Dlugokencky, E. and Tans, P.: Trends in atmospheric carbon dioxide, national Oceanic & Atmospheric Administration, Earth System Research Laboratory (NOAA/ESRL), available at: <http://www.esrl.noaa.gov/gmd/ccgg/trends/global.html>, last access: 9 March 2018, 2018.
- Durbin, J. and Koopman, S. J.: Time series analysis by state space methods, 38, Oxford University Press, 2012.
- 15 Durbin, J. and Watson, G. S.: Testing for Serial Correlation in Least Squares Regression, *Biometrika*, 58, 1 – 19, 1971.
- Gloor, M., Sarmienti, J. L., and Gruber, N.: What can be learned about carbon cycle climate feedbacks from the CO₂ airborne fraction?, *Atmospheric Chemistry and Physics*, 10, 7739 – 7751, 2010.
- Granger, C. W. J. and Newbold, P.: Spurious regression in econometrics, *Journal of Econometrics*, 2, 111 – 120, 1974.
- Hansis, E., Davis, S. J., and Pongratz, J.: Relevance of methodological choices for accounting of land use change carbon fluxes, *Global
20 Biogeochem. Cy.*, 29, 1230 – 1246, 2015.
- Houghton, R. A. and Nassikas, A. A.: Global and regional fluxes of carbon from land use and land cover change 1850-2015, *Global Biogeochem. Cy.*, 31, 456 – 472, 2017.
- Jarque, C. M. and Bera, A. K.: A Test for Normality of Observations and Regression Residuals, *International Statistical Review*, 2, 163–172, 1987.
- 25 Knorr, W.: Is the airborne fraction of anthropogenic CO₂ emissions increasing?, *Geophysical Research Letters*, 36, 2009.
- Le Quééré, C., Andrew, R. M., Friedlingstein, P., Sitch, S., Pongratz, J., Manning, A. C., Korsbakken, J. I., Peters, G. P., Canadell, J. G., Jackson, R. B., Boden, T. A., Tans, P. P., Andrews, O. D., Arora, V. K., Bakker, D. C. E., Barbero, L., Becker, M., Betts, R. A., Bopp, L., Chevallier, F., Chini, L. P., Ciais, P., Cosca, C. E., Cross, J., Currie, K., Gasser, T., Harris, I., Hauck, J., Haverd, V., Houghton, R. A., Hunt, C. W., Hurtt, G., Ilyina, T., Jain, A. K., Kato, E., Kautz, M., Keeling, R. F., Klein Goldewijk, K., Körtzinger, A., Landschützer, P.,
30 Lefèvre, N., Lenton, A., Lienert, S., Lima, I., Lombardozzi, D., Metzl, N., Millero, F., Monteiro, P. M. S., Munro, D. R., Nabel, J. E. M. S., Nakaoka, S.-I., Nojiri, Y., Padin, X. A., Pregon, A., Pfeil, B., Pierrot, D., Poulter, B., Rehder, G., Reimer, J., Rödenbeck, C., Schwinger, J., Séférian, R., Skjelvan, I., Stocker, B. D., Tian, H., Tilbrook, B., Tubiello, F. N., van der Laan-Luijkx, I. T., van der Werf, G. R., van Heuven, S., Viovy, N., Vuichard, N., Walker, A. P., Watson, A. J., Wiltshire, A. J., Zaehle, S., and Zhu, D.: Global Carbon Budget 2017, *Earth System Science Data*, 10, 405–448, <https://doi.org/10.5194/essd-10-405-2018>, <https://www.earth-syst-sci-data.net/10/405/2018/>,
35 2018.
- Le Quééré, C., Raupach, M. R., Canadell, J. G., Marland, G., Bopp, L., Ciais, P., Conway, T. J., Doney, S. C., Feely, R. A., Foster, P., Friedlingstein, P., Gurney, K., Houghton, R. A., House, J. I., Huntingford, C., Levy, P. E., Lomas, M. R., Majkut, J., Metzl, N., Ometto,



- J. P., Peters, G. P., Prentice, I. C., Randerson, J. T., Running, S. W., Sarmiento, J. L., Schuster, U., Sitch, S., Takahashi, T., Viovy, N., van der Werf, G. R., and Woodward, F. I.: Trends in the sources and sinks of carbon dioxide, *Nature Geoscience*, 2, 831 – 836, 2009.
- Raupach, M. R.: The exponential eigenmodes of the carbon-climate system, and their implications for ratios of responses to forcings, *Earth System Dynamics*, 4, 31 – 49, 2013.
- 5 Raupach, M. R., Canadell, J. G., and Quéré, C. L.: Anthropogenic and biophysical contributions to increasing atmospheric CO₂ growth rate and airborne fraction, *Biogeosciences*, 5, 1601 – 1613, 2008.
- Raupach, M. R., Gloor, M., Sarmiento, J. L., Canadell, J. G., Frölicher, T. L., Gasser, T., Houghton, R. A., Le Quéré, C., and Trudinger, C. M.: The declining uptake rate of atmospheric CO₂ by land and ocean sinks, *Biogeosciences*, 11, 3453–3475, <https://doi.org/10.5194/bg-11-3453-2014>, <https://www.biogeosciences.net/11/3453/2014/>, 2014.